

1972

# Applications of the Polarized-Orbital Method: I. Slow Electron-Scattering From Neon and Agron. II. Photoionization Cross-Sections of Sodium and Potassium.

Edward Andrew Garbaty

*Louisiana State University and Agricultural & Mechanical College*

Follow this and additional works at: [https://digitalcommons.lsu.edu/gradschool\\_disstheses](https://digitalcommons.lsu.edu/gradschool_disstheses)

---

## Recommended Citation

Garbaty, Edward Andrew, "Applications of the Polarized-Orbital Method: I. Slow Electron-Scattering From Neon and Agron. II. Photoionization Cross-Sections of Sodium and Potassium." (1972). *LSU Historical Dissertations and Theses*. 2339.  
[https://digitalcommons.lsu.edu/gradschool\\_disstheses/2339](https://digitalcommons.lsu.edu/gradschool_disstheses/2339)

This Dissertation is brought to you for free and open access by the Graduate School at LSU Digital Commons. It has been accepted for inclusion in LSU Historical Dissertations and Theses by an authorized administrator of LSU Digital Commons. For more information, please contact [gradetd@lsu.edu](mailto:gradetd@lsu.edu).

## INFORMATION TO USERS

This dissertation was produced from a microfilm copy of the original document. While the most advanced technological means to photograph and reproduce this document have been used, the quality is heavily dependent upon the quality of the original submitted.

The following explanation of techniques is provided to help you understand markings or patterns which may appear on this reproduction.

1. The sign or "target" for pages apparently lacking from the document photographed is "Missing Page(s)". If it was possible to obtain the missing page(s) or section, they are spliced into the film along with adjacent pages. This may have necessitated cutting thru an image and duplicating adjacent pages to insure you complete continuity.
2. When an image on the film is obliterated with a large round black mark, it is an indication that the photographer suspected that the copy may have moved during exposure and thus cause a blurred image. You will find a good image of the page in the adjacent frame.
3. When a map, drawing or chart, etc., was part of the material being photographed the photographer followed a definite method in "sectioning" the material. It is customary to begin photoing at the upper left hand corner of a large sheet and to continue photoing from left to right in equal sections with a small overlap. If necessary, sectioning is continued again — beginning below the first row and continuing on until complete.
4. The majority of users indicate that the textual content is of greatest value, however, a somewhat higher quality reproduction could be made from "photographs" if essential to the understanding of the dissertation. Silver prints of "photographs" may be ordered at additional charge by writing the Order Department, giving the catalog number, title, author and specific pages you wish reproduced.

### University Microfilms

300 North Zeeb Road  
Ann Arbor, Michigan 48106  
A Xerox Education Company

73-13,663

GARBATY, Edward Andrew, 1930-  
APPLICATIONS OF THE POLARIZED-ORBITAL METHOD:  
I. SLOW ELECTRON SCATTERING FROM NEON AND  
AGRON. II. PHOTOIONIZATION CROSS SECTIONS OF  
SODIUM AND POTASSIUM.

The Louisiana State University and Agricultural  
and Mechanical College, Ph.D., 1972  
Physics, atomic

University Microfilms, A XEROX Company, Ann Arbor, Michigan

- APPLICATIONS OF THE POLARIZED-ORBITAL METHOD:  
I. SLOW ELECTRON SCATTERING FROM NEON AND ARGON  
II. PHOTOIONIZATION CROSS SECTIONS OF SODIUM AND POTASSIUM

A Dissertation

Submitted to the Graduate Faculty of the  
Louisiana State University and  
Agricultural and Mechanical College  
in partial fulfillment of the  
requirements for the degree of  
Doctor of Philosophy

in

The Department of Physics and Astronomy

by  
Edward Garbaty  
A.B., Rutgers University, 1953  
M.S., Iowa State University, 1959  
December, 1972

**PLEASE NOTE:**

Some pages may have

indistinct print.

Filmed as received.

**University Microfilms, A Xerox Education Company**

## ACKNOWLEDGEMENTS

The author wishes to express his deepest appreciation to Dr. R. W. LaBahn for his supervision of my graduate research.

The author is indebted to the L.S.U. Computer Research Center for making available the needed computational facilities.

Financial assistance received from the "Dr. Charles E. Coates Memorial Fund of the LSU Foundation" for the publication of this work is gratefully acknowledged.

Finally, I would like to dedicate this dissertation to my wife and parents in gratitude for their encouragement.

# TABLE OF CONTENTS

	Page
ACKNOWLEDGEMENTS . . . . .	ii
LIST OF TABLES . . . . .	iv
LIST OF FIGURES . . . . .	v
ABSTRACT . . . . .	vi
PART I: SLOW ELECTRON SCATTERING FROM NEON AND ARGON	1
I-1. INTRODUCTION . . . . .	2
I-2. PERTURBATION THEORY FORMALISM . . . . .	5
I-3. STERNHEIMER AND SLATER APPROXIMATIONS . . . . .	9
I-4. RESULTS AND DISCUSSIONS . . . . .	15
PART II: PHOTOIONIZATION CROSS SECTIONS OF SODIUM AND	
POTASSIUM . . . . .	28
II-1. INTRODUCTION . . . . .	29
II-2. REPRESENTATION OF INITIAL AND FINAL STATES . . . . .	31
II-3. MATRIX ELEMENTS . . . . .	36
II-4. RESULTS . . . . .	41
II-5. CONCLUSIONS . . . . .	44
REFERENCES . . . . .	55
VITA . . . . .	57

# LIST OF TABLES

Table	Page
I Contributions to the dipole polarizability for neon	19
II Contributions to the dipole polarizability for argon	20
III Neon scattering lengths by various approximations	21
IV Argon scattering lengths by various approximations	22
V Electron-neon partial-wave phase shifts from the Slater approximations	23
VI Electron-argon partial-wave phase shifts from the Slater approximations	24
VII Contributions to the dipole polarizability associated with the chosen parameter values	46
VIII Calculated valence-electron binding energies and experimental ionization energy	47
IX Non-coulomb p-wave phase shifts	48
X Sodium zeroth-order matrix elements and corrections of first- and second-order in the length (L) and velocity (V) forms for the transitions $s \rightarrow p$ , $p \rightarrow s$ , and $p \rightarrow d$	49
XI Potassium zeroth-order matrix elements and corrections of first- and second-order in the length (L) and velocity (V) forms for the transitions $s \rightarrow p$ , $p \rightarrow s$ , and $p \rightarrow d$	50



## LIST OF FIGURES

Figure	Page
1 Total scattering cross sections for neon	26
2 Total scattering cross sections for argon	27
3 Zeroth- and first-order photoionization cross sections for sodium	52
4 Zeroth- and first-order photoionization cross sections for potassium	53
5 Total (to second-order) photoionization cross sections for sodium	54
6 Total (to second-order) photoionization cross sections for potassium	55

results of the elastic scattering of electrons from neon and argon, the good agreement with experiment of the calculated binding energies of sodium and potassium, and the good agreement of the non-coulomb p-wave phase shifts with those calculated by other methods. It was anticipated that the calculations would behave in a manner similar to what Matese and LaBahn had determined for lithium. A fair agreement between the dipole-length and dipole-velocity results for zero order would be improved as first-order and second-order corrections were added. The first-order corrections, however, were on the same order of magnitude or larger than the zero order values, causing greater disagreement between the dipole-length and dipole-velocity results. Whereas, for lithium the results converged toward the correct value for the photoionization cross section no such indication was given by the results for sodium or potassium. Therefore, the procedure successfully applied to lithium does not have general applicability.

PART I SLOW ELECTRON SCATTERING FROM NEON AND ARGON

## I-1. INTRODUCTION

Recently Matese and LaBahn<sup>1</sup> calculated the photoionization cross section for lithium, wherein they successfully applied the method of polarized orbitals to account for core polarization effects. Their approach was a logical extension of the application by LaBahn and Callaway<sup>2,3</sup> of the polarized orbital method to the analysis of elastic scattering of electrons from helium. A similar approach suggested itself for the case of the heavier alkali metals, the next two being sodium and potassium. The complementary problem which will give some indication of the validity of a polarized orbital calculation on equivalent electronic core configurations, is the analysis of elastic scattering of electrons by neon and argon. The purpose of this part is to present the results of calculations on the elastic scattering of electrons by neon and argon by the polarized-orbital method.

It has been understood for about 40 years that the problem of slow electron scattering by rare gas atoms requires consideration of both exchange and polarization effects. Exchange effects have generally been accounted for by assuming the wave function for the system to be of a properly antisymmetrized form. Polarization effects avoided a simple analysis until about 15 years ago, when the method of polarized orbital was developed.<sup>4</sup> This method, which is applied in this work, determines a polarization potential that accounts for the polarization of the atom by the scattering electron.

In 1966, Thompson<sup>5</sup> analyzed the elastic scattering of electrons by neon and argon, incorporating both exchange and polarization effects. He used a variant of the polarized orbital method known as the adiabatic-exchange approximation. His results were in good agreement with experiment near zero energy and maintained relatively good agreement to an energy of one rydberg. Whereas he considered only the  $np \rightarrow d$  transition, we have examined all the excitations from the outermost orbital for which  $\Delta l = \pm 1$ . Calculations were made in both an unnormalized or normalized manner, depending on whether or not the calculated polarizability was close to the experimental value.

Thompson obtained his polarization potential by determining the polarized orbitals using the Sternheimer approximation. In this calculation the Sternheimer procedure was also utilized and in addition, an alternate one was developed based upon the Slater-averaged-exchange approximation. A comparison of our total cross section results from both procedures is made with those of Thompson and some recent experiments.

The derivation of the pertinent equations, up to the point of applying either the Sternheimer or Slater approximation is given in Section I-2. The formalism of the Sternheimer and Slater approximations appears in Section I-3. Section I-4 contains the results and discussions.

## I-2. PERTURBATION THEORY FORMALISM<sup>6</sup>

In the method of polarized orbitals one seeks to find the first-order correction to the atomic orbitals arising from the perturbation by the electric field of the scattering electron. The only orbitals considered to be perturbed are the outer ones which correspond to the least tightly bound electrons. The extension of the Hartree-Fock (HF) formalism for an unperturbed atom or ion to first-order perturbation theory yields for the form of the one-electron HF equation

$$[h(1) + \lambda h' - \epsilon_i] \chi_i(1) = 0, \quad i = 1, 2, \dots, N, \quad \text{I.1}$$

where the spin orbitals  $\chi_i$  are orthonormal; that is,

$$\langle \chi_i | \chi_j \rangle = \delta_{ij}, \quad i, j = 1, 2, \dots, N. \quad \text{I.2}$$

In Eq. I.1,  $h(1)$  is the one-electron HF operator which for an atom of charge  $Z$  takes the form

$$h(1) = -\nabla_1^2 - ZZ/r_1 + \sum_{j=1}^N 2 \langle \chi_j | r_{12}^{-1} (1 - \rho_{12}) | \chi_j \rangle, \quad \text{I.3}$$

$h'$  represents the perturbation  $(2|\vec{r}_1 - \vec{r}_e|^{-1})$  in our case, with  $\vec{r}_e$  as the coordinate of the perturbing charge), and  $\lambda$  serves as the usual perturbation theory expansion parameter which is later set equal to 1. The operator in the summation in Eq. I.3 signifies

$$\begin{aligned} \langle \chi_j | r_{12}^{-1} (1 - \rho_{12}) | \chi_j \rangle f(1) &= f(1) \int \chi_j^*(2) r_{12}^{-1} \chi_j(2) d\tau_2 \\ &- \chi_j(1) \int \chi_j^*(2) r_{12}^{-1} f(2) d\tau_2, \end{aligned} \quad \text{I.4}$$

where  $f(1)$  is an arbitrary function of the space and spin coordinates of electron 1.

Introducing a perturbation expansion, one writes

$$\chi_i = \chi_i^{\circ} + \lambda \chi_i' + \dots \quad \text{I.5}$$

$$\epsilon_i = \epsilon_i^{\circ} + \lambda \epsilon_i' + \dots \quad \text{I.6}$$

which upon substitution in Eq. I.1 yields for the zeroth and first order in  $\lambda$ , respectively,

$$[h^{\circ}(1) - \epsilon_i^{\circ}] \chi_i^{\circ}(1) = 0, \quad \text{I.7}$$

$$\begin{aligned} [h^{\circ}(1) - \epsilon_i^{\circ}] \chi_i'(1) + [h' - \epsilon_i'] \chi_i^{\circ}(1) + \sum_{j=1}^N 2 [\langle \chi_j' | \eta_{12}^{-1} (1 - P_{12}) | \chi_j^{\circ} \rangle \\ + \langle \chi_j^{\circ} | \eta_{12}^{-1} (1 - P_{12}) | \chi_j' \rangle] \chi_i^{\circ}(1) = 0, \end{aligned} \quad \text{I.8}$$

where  $h^{\circ}(1)$  is the zeroth-order HF operator

$$h^{\circ}(1) = -\nabla_1^2 - 2Z/r_1 + \sum_{j=1}^N 2 \langle \chi_j^{\circ} | \eta_{12}^{-1} (1 - P_{12}) | \chi_j^{\circ} \rangle. \quad \text{I.9}$$

This operator has solutions  $\chi_i^{\circ}$  which are the usual HF orbitals and obey the orthonormality relation

$$\langle \chi_i^{\circ} | \chi_j^{\circ} \rangle = \delta_{ij}, \quad i, j = 1, 2, \dots, N. \quad \text{I.10}$$

The first-order equation, Eq. I.8, will yield  $\epsilon_i'$ , once  $\chi_i'$  is found, by multiplication on the left by  $\chi_i^{\circ}(1)$  and integrating over the coordinates of electron 1. This first-order coupled HF equation has been solved by others,<sup>7</sup> who report the effort to be very time consuming. The problem of finding a satis-

factory approximation to the solution can be expedited by neglecting all of the terms which represent essentially small effects but add considerable complication.

One of the simplest uncoupling procedures, first suggested by Dalgarno,<sup>8</sup> is to neglect in Eq. I.8 all terms in the sum over  $j$ . This results in the equation

$$[h^0(i) - \epsilon_i^0] \chi_i'(i) + [h' - \epsilon_i'] \chi_i^0(i) = 0. \quad \text{I.11}$$

Another uncoupling procedure which is equally convenient was suggested by Langhoff, Karplus, and Hurst.<sup>7</sup> We first rearrange Eq. I.8 and write it in the form

$$[h_i^0(i) - \epsilon_i^0] \chi_i'(i) + [h' - \epsilon_i'] \chi_i^0(i) + \sum_{j=1}^N (j \neq i) 2 [\langle \chi_j' | h_{12}' (1 - P_{12}) | \chi_j^0 \rangle + \langle \chi_j^0 | h_{12}' (1 - P_{12}) | \chi_j' \rangle] \chi_i^0(i) = 0, \quad \text{I.12}$$

where the operator  $h_i^0(1)$  acting on  $\chi_i'$  is

$$h_i^0(i) = -\nabla_i^2 - 2Z/r_i + \sum_{j=1}^N (j \neq i) 2 \langle \chi_j^0 | h_{12}' (1 - P_{12}) | \chi_j^0 \rangle. \quad \text{I.13}$$

One should note that Eqs. I.8 and I.12 are equivalent, since in Eq. I.8 the term ( $j=i$ ) in the explicit sum over  $j$  cancels the self-potential term ( $j=i$ ) in  $h^0(1)$ . The terms with  $j \neq i$  in Eq. I.12, known as the first-order self-consistency correction, are now dropped to simplify the equation. This will eliminate all the terms involving first-order functions  $\chi_j'$  other than the one being calculated ( $\chi_i'$ ), thus uncoupling the equation and leaving the expression



$$[\mathcal{H}_i^{\circ}(1) - \epsilon_i^{\circ}] \chi_i^{\prime}(1) + [\mathcal{H}' - \epsilon_i^{\prime}] \chi_i^{\circ}(1) = 0. \quad \text{I.14}$$

This differs from Eq. I.11 in having a modified operator  $h_i^{\circ}(1)$  [Eq. I.13].

Langhoff et al.<sup>7</sup> have solved these three approximations, including the fully coupled equation I.8, and together with yet a fourth approximation have applied the solutions to calculate the dipole and quadrupole polarizabilities and shielding factors of various atoms and ions. Their results show that the approximation represented by Eq. I.14 is significantly better than that of Eq. I.11, in that it gives values that are in good agreement with those obtained from the fully coupled equation which are expected to be most accurate.

### I-3. STERNHEIMER AND SLATER APPROXIMATIONS

Equations I.11 and I.14 are still complex enough to warrant some further approximations that would ease the computational problem. The first approximation we have considered is what is commonly known as the Sternheimer approximation.<sup>9</sup> To exhibit the nature of this approximation it is necessary to be more specific in the representation of the spin orbitals. Hence, let

$$\chi_i^0(l) = (u_{nl}(r_1)/r_1) Y_l^m(\theta, \varphi) \sigma(i) \quad \text{I.15}$$

$$\chi_i^l(l) = \sum_{l'm'} (u_{nl \rightarrow l'}(r_1, R)/r_1) C_{nl \rightarrow l'}^{m \rightarrow m'} Y_{l'}^{m'}(\theta, \varphi) \sigma(i). \quad \text{I.16}$$

The subscripts in  $u_{nl \rightarrow l'}$  exhibit explicitly that the excitation of the electron is from a state of orbital angular momentum  $l$  to one of  $l'$ . Simplifying the notation, let the operator

$$h^0(l) - \epsilon_i^0 = -\nabla_l^2 + V_0 - \epsilon_{nl} \quad \text{I.17}$$

Operating with this on the unperturbed spin orbital one can separate out the radial equation

$$\left( -\frac{d^2}{dr^2} + \frac{l(l+1)}{r^2} + V_0 - \epsilon_{nl} \right) u_{nl} = 0, \quad \text{I.18}$$

from which one can make the association

$$\frac{l(l+1)}{r^2} + V_0 \frac{u_{nl}}{u_{nl}} - \epsilon_{nl} = \frac{u_{nl}''}{u_{nl}} \quad \text{I.19}$$

Correspondingly, operating on the perturbed spin orbital one

obtains for the radial part of Eq. I.11

$$\left( \frac{d^2}{dn^2} + \frac{l'(l'+1)}{n^2} + V_0 - \epsilon_{nl} \right) u_{nl \rightarrow l'} = - \frac{2n\epsilon}{n^2} u_{nl}, \quad \text{I.20}$$

where on the right-hand side we have the expression corresponding to a dipole approximation for the perturbation term. Using Eq. I.19 one can approximate Eq. I.20 as

$$\left[ \frac{d^2}{dn^2} + \frac{l'(l'+1) - l(l+1)}{n^2} + \frac{1}{u_{nl}} \frac{d^2}{dn^2} u_{nl} \right] u_{nl \rightarrow l'} = - \frac{2n\epsilon}{n^2} u_{nl}. \quad \text{I.21}$$

In this form the equation is readily solved numerically for  $u_{nl \rightarrow l'}$ , where  $u_{nl}$  can be taken to be HF self-consistent field functions tabulated by Clementi.<sup>10</sup>

Now a second approach, which we call the Slater approximation, arises by the use of Eq. I.14. Langhoff et al.<sup>7</sup> point out that care must be exercised in its application to different systems. For our case of a closed-shell system of  $2N$  electrons in  $N$  doubly occupied orbitals, Eq. I.14 should be replaced with

$$[f_i^0(i) - \epsilon_i^0] \psi_i'(i) + [h' - \epsilon_i'] \psi_i^0(i) = 0, \quad \text{I.22}$$

where  $\psi$  is the spatial part of the atomic orbitals ( $\chi_i = \psi_i \sigma(i)$ ) and

$$\begin{aligned} f_i^0(i) = & -\nabla_i^2 - 2Z/n_i + \sum_{j=1}^N (j \neq i) 2 \langle \psi_j^0 | n_{i2}^{-1} (2 - P_{i2}) | \psi_j^0 \rangle \\ & + 2 \langle \psi_i^0 | n_{i2}^{-1} (1 + 2 P_{i2}) | \psi_i^0 \rangle. \end{aligned} \quad \text{I.23}$$

An expansion of the sum and recombination of the terms permits one to express the form of the operator as

$$\begin{aligned}
\phi_i^o(1) = & -\nabla_1^2 - 2z/\eta_1 + \sum_{j=1}^{N'} \int |\psi_j^o(2)|^2 \psi_{\eta_{12}} d\tau_2 \\
& - \sum_{j=1}^N (j \neq i) \langle \psi_j^o | 2\eta_{12}^{-1} P_{12} | \psi_j^o \rangle + 2 \langle \psi_i^o | 2\eta_{12}^{-1} P_{12} | \psi_i^o \rangle. \quad \text{I.24}
\end{aligned}$$

Adding and subtracting  $2 \sum_{j=1}^N (j \neq i) \langle \psi_j^o | 2\eta_{12}^{-1} P_{12} | \psi_j^o \rangle$  puts the operator in the form

$$\begin{aligned}
\phi_i^o(1) = & -\nabla_1^2 - 2z/\eta_1 + \sum_{j=1}^{N'} \int |\psi_j^o(2)|^2 \psi_{\eta_{12}} d\tau_2 \\
& + 2 \sum_{j=1}^N \langle \psi_j^o | 2\eta_{12}^{-1} P_{12} | \psi_j^o \rangle - \frac{3}{2} \left[ 2 \sum_{j=1}^N (j \neq i) \langle \psi_j^o | 2\eta_{12}^{-1} P_{12} | \psi_j^o \rangle \right] \quad \text{I.25}
\end{aligned}$$

Employing Slater's approximation of the exchange operator term,  $2 \sum_{j=1}^N \langle \psi_j^o | 2\eta_{12}^{-1} P_{12} | \psi_j^o \rangle$ , by  $6 \left[ \frac{3}{8\pi} \sum_j^{3N} \chi_j^*(1) \chi_j(1) \right]^{1/3}$  and labeling it  $A_S$ ; one can then write

$$\phi_i^o(1) - \varepsilon_i^o = -\nabla_1^2 + V' + \lambda (A_S - \frac{3}{2} A_S'') - \varepsilon_{me}, \quad \text{I.26}$$

where

$$V' = -2z/\eta_1 + \sum_{j=1}^{N'} \int |\psi_j^o(2)|^2 \psi_{\eta_{12}} d\tau_2, \quad \text{I.27}$$

and  $\lambda$  is a parameter, the value of which will be discussed later. The single prime implies that one excludes from the sum the electron that is in the orbital being perturbed. The double prime implies that two electrons in the orbital being perturbed are excluded from the sum.  $A_S$  is the well known Slater-averaged-exchange potential originally computed as the exchange correction in a free-electron gas model.<sup>11</sup> The particular combination that arises in the operator Eq. I.26 stems from the need to preserve spherical symmetry.

Using the operator in the form of Eq. I.26 in expression Eq. I.22, one obtains the radial equation

$$\left(-\frac{d^2}{dr^2} + \frac{l'(l'+1)}{r^2} + V' + \lambda(A_s - \frac{1}{2} A_s'') - \epsilon_{ml}\right) u_{ml \rightarrow l'} = -\frac{2\eta_c}{r^2} u_{ml}, \quad \text{I.28}$$

where again the perturbation term on the right-hand side is taken in the dipole approximation. In this form the equation is solved numerically for  $u_{ml \rightarrow l'}$ , with the  $u_{ml}$  again taken as the functions tabulated by Clementi.<sup>10</sup>

For a comparison of these two approximations, the respective solutions were used to calculate the dipole polarizabilities and the total elastic scattering cross sections. The dipole polarizability is obtained from the expression

$$\alpha_{ml \rightarrow l'} = C_{l \rightarrow l'} \int_0^\infty u_{ml} u_{ml \rightarrow l'} r dr, \quad \text{I.29}$$

where  $C_{l \rightarrow l'}$  accounts for all constants and angular integrations. The results are tabulated in Tables I and II and discussed in Section I-4.

In order to determine the scattering cross section one needs phase shifts which are obtained from the solution of a scattering equation for the reduced radial wave function of the scattered electron. The appropriate scattering equation is, in the notation used by Thompson,<sup>5</sup>

$$(L+k^2)F_{kl}(R) = K F_{kl}(R) + \sum_m (k^2 + \epsilon_{ml}) \int_0^\infty u_{ml}(r') F_{kl}(r') dr' u_{ml}(R), \quad \text{I.30}$$

where

$$L = \frac{d^2}{2R^2} + \frac{2}{R} - \frac{1}{R} \sum_{m \neq l} 4(2l+1) Y_0(u_{ml}, u_{ml}) - \frac{L(L+1)}{R^2} + V_p(R). \quad \text{I.31}$$

The polarization potential  $V_p$  is given by

$$V_p(R) = \sum_j \int \chi_j^0(\vec{r}_1) \frac{2\lambda_j}{\lambda_j^2} \cos \theta \chi_j'(\vec{r}_1, R) d\vec{r}_1. \quad \text{I.32}$$

The other terms and symbols in Eqs. I.31 and I.32 are defined as

$$K_{F_{kl}}(R) = -\frac{1}{R} \sum_{m \neq l} (2l+1) C_{lL\lambda} Y_\lambda(u_{ml}, F_{kl}) u_{ml}(R), \quad \text{I.33}$$

$$Y_\lambda(A, B) = R^{-\lambda} \int_0^R A(r) B(r) r^\lambda dr + R^{\lambda+1} \int_R^\infty A(r) B(r) r^{-\lambda-1} dr, \quad \text{I.34}$$

$$C_{lL\lambda} = \int_{-1}^1 P_l(x) P_L(x) P_\lambda(x) dx, \quad \text{I.35}$$

with  $P_l$  representing the Legendre polynomial of order  $l$ .

In the numerical solution of Eqs. I.22, I.28, and I.30, all iterations were performed using Numerov's method. All integrals were evaluated by means of the trapezoidal rule. The starting values required were obtained by appropriate power-series expansion of the functions. In the iterations a variable mesh size was used that began with  $\Delta r = 0.0025a_0$  at the origin and doubled periodically to  $\Delta r = 0.16a_0$  at  $r = 25.0a_0$ , remaining at this value for all larger  $r$ . The phase shifts were determined by employing a procedure due to Burgess,<sup>12</sup> with the iteration extended until the value converged to within  $5 \times 10^{-5}$  rad. This occurred usually in the neighborhood of  $r = 35a_0$ . Having determined the phase shifts, the total elastic scattering cross section is calculated from the

expression

$$Q = (4/k^2) \sum_L (2L+1) \sin^2 \eta_L . \quad \text{I.36}$$

The range of the partial-wave sum for neon was  $L=0,1,2$  and for argon  $L=0,1,2,3$ . Some of the partial-wave shifts and scattering cross section results are presented in the following section.

#### I-4. RESULTS AND DISCUSSIONS

Contributions to the dipole polarizability from the outermost occupied level are listed for neon in Table I and for argon in Table II. They are compared with earlier calculations by Kaneko,<sup>13</sup> who used the Sternheimer approximation, and experiment. Our Sternheimer results for neon are in better agreement with experiment than Kaneko's. In addition, the Sternheimer components calculated by Montgomery and LaBahn<sup>14</sup> in an independent calculation agree with the present calculations.

Results for argon were not as satisfying in that no significant change in the values of the polarizabilities in Sternheimer approximation were obtained from those of Kaneko<sup>13</sup> or Montgomery and LaBahn.<sup>14</sup> The change in the total polarizability through use of the Slater approximation also went the wrong way and did not yield the desirable reduction that occurred for neon.

The additional sets of values listed correspond to some of the modifications made to the Slater approximation. The nature of these modifications will be described later. The seven modifications being reported for which the total scattering cross sections were calculated are listed in Table III. This table gives a comparison of the total polarizability with the zero-energy scattering length for argon. The analogous results for neon are exhibited in Table IV. The scattering lengths were observed to be quite sensitive to the value of the total polarizability, in a given approxima-



tion.

The total scattering cross sections were generally calculated at energies in the range 0.00 to 1.00 rydbergs at increments of 0.10 rydbergs. A few additional values were calculated in the neighborhood of the maximum and minimum for the Slater  $\times 0.594$  modification. As was mentioned earlier, all calculations included the three transitions  $ns \rightarrow p$ ,  $np \rightarrow s$ , and  $np \rightarrow d$ , where  $n$  has the value corresponding to the outermost occupied level. The partial phase shifts are listed for only a few modifications, viz., those for neon in Table V and argon in Table VI.

Let us now consider the nature of the modifications used. If the calculated value of the polarizability was significantly different from the experimental one, a second solution of the scattering equation was made using a polarization potential normalized to the experimental value of the polarizability. The normalizing factors were just the ratio of the experimental to calculated values of the polarizability. The results are labeled appropriately as unnormalized and normalized.

Another modification was made to the Slater approximation of the exchange term in the potential. Slater<sup>11</sup> derived his averaged-exchange potential on the basis of a free-electron-gas model. More recently Kohn and Sham<sup>15</sup> in their consideration of the problem of a homogeneous gas of interacting electrons have obtained the same functional form except reduced by a factor of  $1/3$ . Slater has found a conve-

nient approximation for the exchange interaction which may be successfully applied to different systems, with more than just a few electrons, by suitably choosing a multiplicative strength parameter. Calculations were made with the factor taken as both six and four, and the corresponding results labeled as Slater and Slater  $\times 2/3$ . One would have hoped that the better agreement with the experimental results would have decided which factor was more correct.

The good agreement of the Slater cross sections for neon with the recent experimental results of Salop and Nakano<sup>16</sup> shown in Fig. 1 would indicate the factor of six as being better. Although no improvement was expected, the modifications Slater  $\times 2/3$  (UNNORM) and Slater  $\times 2/3$  (NORM) were calculated for neon to observe the relative behavior when they are applied to argon.

The argon results shown in Fig. 2 imply in contradiction that the factor of four will yield results in better agreement with experiment. Argon results for Slater  $\times 2/3$  are not plotted because they are almost identical with Thompson's above 5 eV and our Sternheimer (NORM) below 5 eV. Since the Slater  $\times 2/3$  modification did not yield the experimental polarizability it was used in a normalized calculation as described above.

The polarizability obtained from the Slater  $\times 2/3$  approximation was considerably improved over the value arising from the Slater approximation. This suggested an alternative normalization procedure, that of multiplying the Slater-

averaged-exchange potential by an appropriate factor which would yield a polarizability equal to the experimental value. A justification for this procedure stems from the fact that the multiplicative factor is dependent on the type of system that is being described. The factors of six or four arise from consideration of systems of a free-electron gas or a homogeneous gas of interacting electrons and should not be expected to be correct in describing the electron distribution in an isolated atom. The results of this calculation, labeled Slater  $\times 0.594$ , are in best agreement with experiment, which is represented in Fig. 2 by the open circles. No further improvement on the agreement however was attempted by an arbitrary manipulation of the factor. Thompson's argon results, obtained through a normalized Sternheimer approximation including only the  $3p \rightarrow d$  transition, was in excellent agreement with the Slater  $\times 0.594$  below 2 eV.

A single curve represents the normalized results of the two approximations (Sternheimer and Slater) since they are in essential agreement. There was a slight deviation in the range of 6-10 eV. The normalized Slater  $\times 2/3$  curve for argon was not shown since it essentially paralleled the Slater  $\times 0.594$  curve, lying above it except for the range between 1 and 5 eV where it dips slightly below.

The behavior of the argon results leads one to conclude that the two different approximations in the normalized modification account for those aspects of the scattering process known as adiabatic-exchange effects. The nature of the dis-

agreement with experiment indicates that some nonadiabatic effects are making an appreciable contribution. The formalism for accounting the nonadiabatic effects has been established and successfully applied to helium<sup>3</sup>. The procedure is known as the extended polarization approximation.

An analysis of the extended polarization approximation has established that the nonadiabatic effects add a repulsive contribution via a distortion potential. This has been shown to be less significant at larger distances than the polarization potential but comparable in the vicinity of the core. Hence, only those scattered electrons that penetrate the core, which are those of the higher energies, will be appreciably affected. The agreement of the results at the lower energies and the appreciable deviation at the higher energies suggests that argon would be an ideal system for testing the extended polarization approximation. Its application would however be difficult and for our ultimate application of this formalism to photoionization of Na and K, the adiabatic-dipole approximation is believed to be sufficiently accurate.

TABLE I: Contributions to the dipole polarizability  
for neon

Approximation	Sternheimer <sup>a</sup>	Sternheimer <sup>b</sup>	Slater	Slater x 2/3
2s→p	1.526	1.330	1.088	0.980
2p→s	0.162	-0.700	-0.917	-1.342
2p→d	2.465	2.148	2.264	2.150
Total	4.153	2.778	2.435	1.788
Experimental <sup>a</sup>	2.687	(units $a_0^3$ )		

<sup>a</sup> Kaneko (Ref. 13)

<sup>b</sup> Present

TABLE II: Contributions to the dipole polarizability for argon

Approximation	Sternheimer <sup>a</sup>	Sternheimer <sup>b</sup>	Slater	Slater x 2/3	Slater x 0.594
3s→p	5.598	5.888	5.070	4.224	4.076
3p→s	-3.282	-3.374	-3.467	-6.255	-7.075
3p→d	13.883	13.998	16.875	14.435	14.000
Total	16.199	16.512	18.478	12.404	11.001
Experimental <sup>a</sup>	11.000	(units $a_0^3$ )			

<sup>a</sup> Kaneko (Ref. 13)

<sup>b</sup> Present

TABLE III: Argon scattering lengths by various approximations (in a.u.)

Approximation	Polarizability	Scattering Length
Slater (UNNORM)	18.48	-8.062
Sternheimer (UNNORM)	16.51	-5.819
Slater x 2/3 (UNNORM)	12.40	-2.327
Sternheimer (NORM)	11.00	-1.946
Slater (NORM)	11.00	-1.898
Slater x 2/3 (NORM)	11.00	-1.689
Slater x 0.594	11.00	-1.608
Thompson <sup>a</sup>	11.00	-1.60
Golden & Bandel (exp) <sup>b</sup>		-1.647

<sup>a</sup> Ref. 5

<sup>b</sup> Ref. 17

TABLE IV: Neon scattering lengths by various approximations (in a.u.)

Approximation	Polarizability	Scattering Length
Slater x 2/3 (UNNORM)	1.79	0.4351
Thompson <sup>a</sup>	2.20	0.347
Slater	2.44	0.2757
Slater x 2/3 (NORM)	2.69	0.0556
Sternheimer	2.78	0.0276
Salop & Nakano (exp) <sup>b</sup>		0.30±0.03

<sup>a</sup> Ref. 5

<sup>b</sup> Ref. 16



TABLE V: Electron-neon partial-wave phase shifts from the Slater approximation (in modulo  $\pi$  radians).

k ( $a_0^{-1}$ )	Energy (eV)	$\eta_0$		$\eta_1$		$\eta_2$	
		A	B	A	B	A	B
0.1	0.136	-0.0468	-0.0583	0.0035	0.0022	0.0008	0.0006
0.2	0.544	-0.1217	-0.1374	0.0071	0.0026	0.0030	0.0023
0.3	1.224	-0.2127	-0.2289	0.0030	-0.0057	0.0070	0.0054
0.4	2.176	-0.3131	-0.3285	-0.0128	-0.0259	0.0131	0.0105
0.5	3.400	-0.4189	-0.4330	-0.0409	-0.0579	0.0219	0.0186
0.6	4.896	-0.5273	-0.5404	-0.0797	-0.0999	0.0342	0.0306
0.7	6.664	-0.6364	-0.6490	-0.1264	-0.1491	0.0504	0.0474
0.8	8.704	-0.7450	-0.7573	-0.1785	-0.2030	0.0708	0.0694
0.9	11.016	-0.8520	-0.8643	-0.2337	-0.2594	0.0956	0.0966
1.0	13.600	-0.9566	-0.9692	-0.2901	-0.3168	0.1245	0.1284

A, Calculated in the HFS (UNNORM) approximation.

B, Calculated in the HFS x 2/3 (UNNORM) approximation.

TABLE VI: Electron-argon partial-wave phase shifts from the Slater approximation (in modulo  $\pi$  radians).

k ( $a_0^{-1}$ )	Energy (eV)	$\eta_0$		$\eta_1$		$\eta_2$		$\eta_3$	
		A	B	A	B	A	B	A	B
0.1	0.136	0.0729	0.0503	0.0158	0.0152	0.0034	0.0034	0.0012	0.0012
0.2	0.544	-0.0039	-0.0374	0.0342	0.0304	0.0143	0.0142	0.0045	0.0045
0.3	1.224	-0.1409	-0.1798	0.0242	0.0142	0.0370	0.0361	0.0100	0.0100
0.4	2.176	-0.3023	-0.3443	-0.0225	-0.0397	0.0820	0.0775	0.0181	0.0180
0.5	3.400	-0.4733	-0.5171	-0.0991	-0.1232	0.1693	0.1535	0.0290	0.0289
0.6	4.896	-0.6467	-0.6917	-0.1955	-0.2256	0.3344	0.2875	0.0435	0.0431
0.7	6.664	-0.8186	-0.8644	-0.3030	-0.3380	0.6238	0.5076	0.0624	0.0613
0.8	8.704	-0.9866	-1.0328	-0.4154	-0.4543	1.0283	0.8181	0.0864	0.0841
0.9	11.016	-1.1492	-1.1956	-0.5288	-0.5707	1.4071	1.1543	0.1163	0.1119
1.0	13.600	-1.3056	-1.3521	-0.6406	-0.6848	1.6611	1.4280	0.1523	0.1447

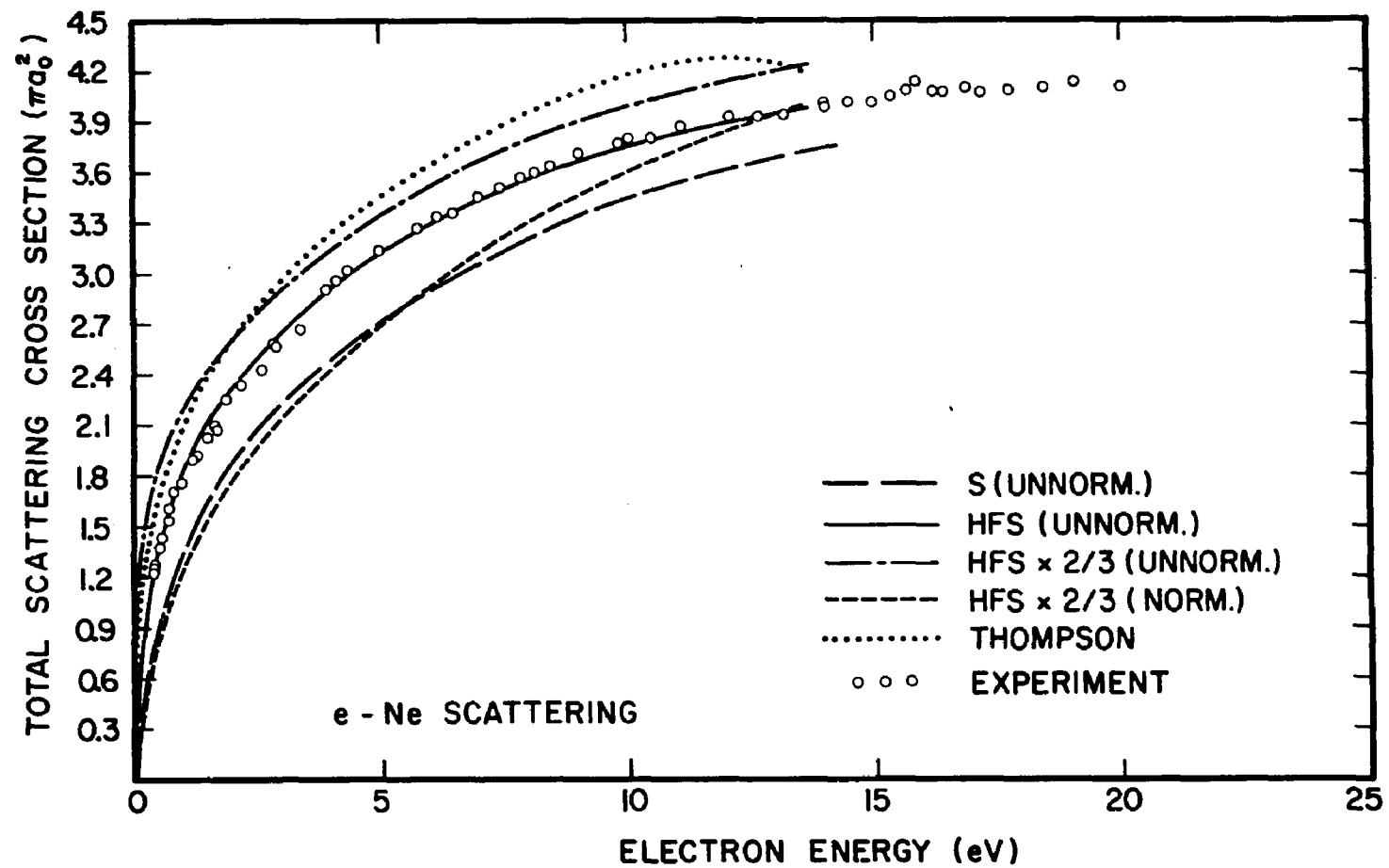
A, Calculated in the HFS (NORM) approximation.

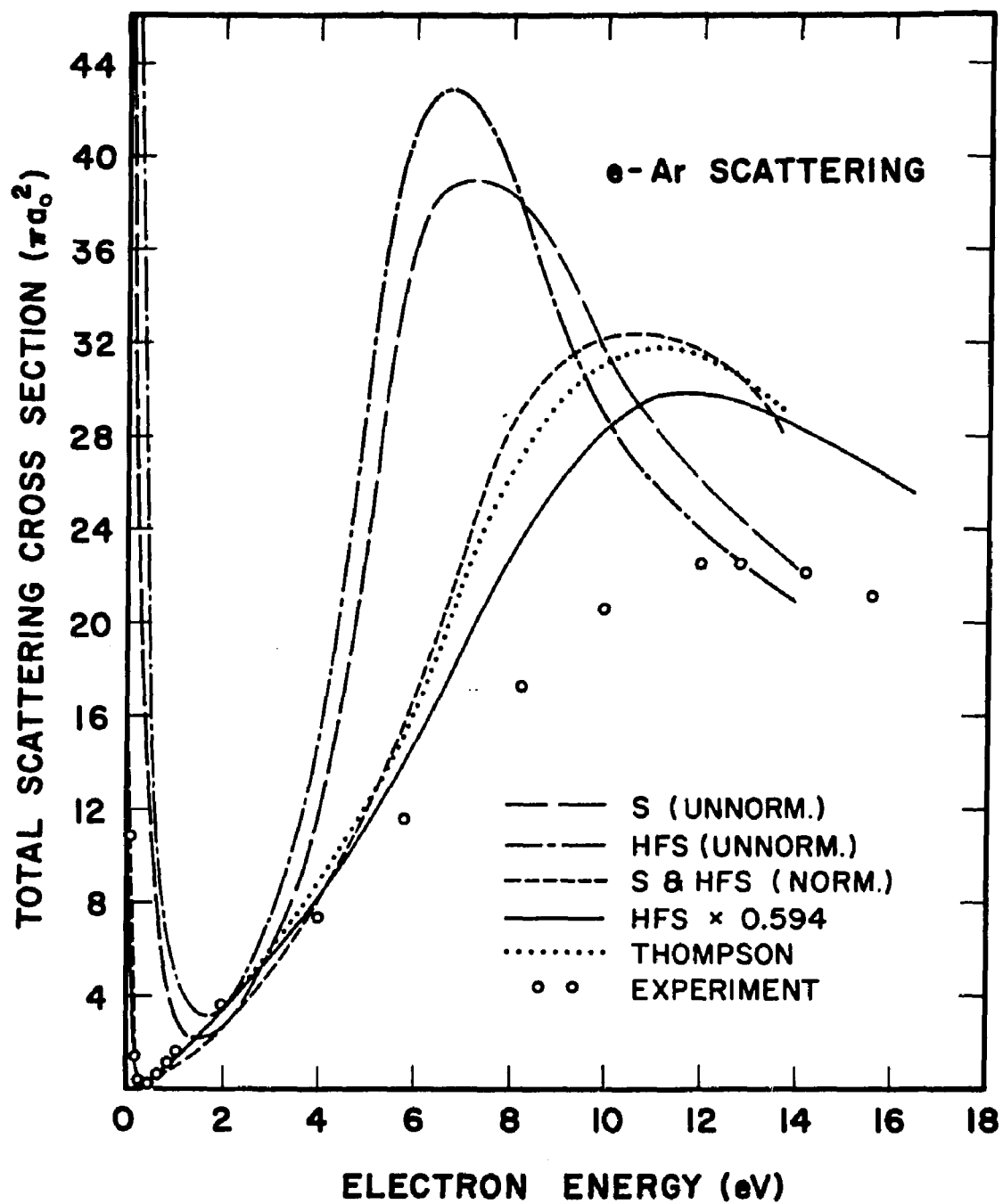
B, Calculated in the HFS x 0.594 approximation.

## FIGURE CAPTIONS

Figure 1: The total scattering cross sections for neon. Our results obtained from various approximations employed in determining the perturbed orbital are compared with the computation of Thompson and the experimental data of Salop and Nakano. The notation designating the different approximations used are: S (UNNORM) for Sternheimer, HFS (UNNORM) for Slater, and  $\text{HFS} \times 2/3$  (UNNORM) for Slater  $\times 2/3$ . The  $\text{HFS} \times 2/3$  (NORM) curve shows the effect of the normalization of the polarization potential obtained from the Slater  $\times 2/3$  approximation.

Figure 2: The total scattering cross sections for argon. Our results obtained from various approximations employed in determining the perturbed orbital are compared with the computation of Thompson and the experimental data of Golden and Bandel. The notation designating the different approximations used are: S (UNNORM) for Sternheimer, HFS (UNNORM) for Slater, and  $\text{HFS} \times 0.594$  for Slater  $\times 0.594$ . The S and HFS (NORM) curve shows the almost identical results obtained by normalizing the polarization potential of either the Sternheimer or Slater approximations.





## PART II PHOTOIONIZATION CROSS SECTIONS OF SODIUM AND POTASSIUM

## II-1. INTRODUCTION

The success of the analysis by Matese and LaBahn<sup>1</sup> of the photoionization cross section for the lithium atom has suggested this application to the alkali metals, sodium and potassium. This calculation of the photoionization cross section by the polarized orbital method will explicitly account for the effect of individual orders of correction, to second order.

The well known formalism for calculating photoionization cross sections<sup>18</sup> requires the evaluation of matrix elements between the initial and final states. Representing these states with exact wave functions permits defining the dipole photoionization cross section in three equivalent ways,<sup>19</sup> known as the dipole-length, dipole-velocity and dipole-acceleration formulae. Calculations have generally been carried out only in the dipole-length and dipole-velocity approximations. The degree of agreement between the results is used as a measure of the exactness of the state wave functions.

Good representation of the state wave functions has been achieved by considering them to be determinantal wave functions, with those elements representing the bound states being taken as fixed-core Hartree-Fock or variationally determined one-electron wave functions. Polarization of the core electrons exists and this has been accounted for by the method of polarized orbitals, primarily by its effect on the continuum wave function. Matese and LaBahn<sup>1</sup> in addition have

incorporated perturbed orbitals for some core states in their representation of the initial and final states. They point out that failing to do so would include some second-order effects in the analysis while neglecting first-order corrections.

Chang and McDowell<sup>20</sup> in their many-body perturbation theory analysis of the photoionization of lithium have determined the relative sizes of various initial and final state corrections. Their results indicate that the second-order final-state correction is dominant in the dipole-length approximation; whereas in the dipole-velocity approximation, it is comparable in magnitude to first-order initial state and first-order final-state corrections. Their results imply that the discrepancies that have existed between calculated photoionization cross sections using the length and velocity approximations may be attributed to the neglect of first-order effects.

In Section II-2 we discuss the representation for the initial and final states. The formalism for computing photoionization cross sections in the dipole-length and dipole-velocity is given in Section II-3. The results are discussed in Section II-4, and the conclusions in Section II-5.



## II-2. REPRESENTATION OF INITIAL AND FINAL STATES

In the case of alkali metals which possess only a single electron over a closed shell core, the total wave function can be represented by a single determinant

$$\Psi = \det |\chi_{\alpha}^{(1)} \chi_{\beta}^{(2)} \dots \chi_{\pi}^{(N)}| / \sqrt{N!} . \quad \text{II.1}$$

The  $\chi_{\alpha}$ ,  $\chi_{\beta}$ , ...,  $\chi_{\pi}$  are one-electron spin orbitals representing the unperturbed and perturbed bound states or a continuum state. Taking the bound state functions representing the core as the corresponding ionic functions tabulated by Clementi<sup>10</sup> will not include any polarization effects.

Designate the spin orbitals that are unperturbed by a zero superscript,  $\chi^0$ , and those perturbed by  $\chi^0 + \chi'$ , where  $\chi'$  are the first-order perturbation corrections of the unperturbed orbitals, determined by the polarized orbital procedure discussed in Section I-3. Expressing the wave function [II.1] in this new notation and then expanding into a linear combination of determinantal functions, we represent the initial and final state wave functions for N electrons as

$$\Psi_{i,f} = \sum_{\text{cyclic}} \sum_p \Psi^{(p)}(1, \dots, Z; x) \varphi_{i,f}(x) / \sqrt{N} , \quad \text{II.2}$$

where the first sum is over a cyclical permutation of the indices and the second over the perturbed orbital components. The  $\varphi_{i,f}$  is the wave function for the valence electron in the initial state,  $\varphi_i = \varphi_{ns}$ , or continuum electron in the final state,  $\varphi_f = \varphi_{kp}$  and  $Z = N-1$ . Four types of wave functions are represented by  $\Psi^{(p)}$ , with

$$\Psi^{(0)} = \det / \chi_{1s}^{(0)} \cdots \chi_{n's \rightarrow p}^{(0)} / \sqrt{Z!} = \bar{\Psi}^{(0)}(1, \dots, Z) \quad \text{II.3}$$

containing only unperturbed core wave functions. The

$$\bar{\Psi}^{(0)} = \det / \chi_{1s}^{(0)} \cdots \chi'_{n's \rightarrow p}(i; x) \cdots / \sqrt{Z!} , \quad \text{II.4}$$

contains the perturbed orbitals for the  $n's \rightarrow p$  transition, and  $\bar{\Psi}^{(2)}$  and  $\bar{\Psi}^{(3)}$ , respectively, those from the  $n'p \rightarrow s$  and  $n'p \rightarrow d$  transitions ( $n' = n-1$ ).

The perturbed orbitals are determined by the procedure described in Section I-3. For this analysis only the ordinary Slater-averaged-exchange approximation was used. Thus, the radial equation [I.28] was slightly modified to the form

$$\left( -\frac{d^2}{dn^2} + \frac{l'(l'+1)}{n^2} + V' + \lambda A_s - \epsilon_{m_l} \right) u_{m_l \rightarrow l'} = -\frac{2\lambda_c}{n^3} u_{m_l} . \quad \text{II.5}$$

The reason for this modification will be explained shortly. All the symbols retain their earlier definition. The  $\lambda$ 's are parameters which are adjusted to yield perturbed orbitals satisfying certain conditions.

In order for the total wave function [Eq. II.2] to be normalized correctly to first-order, the constituent single-electron orbitals must satisfy the following orthogonality conditions<sup>21</sup>

$$\begin{aligned} \langle \chi_i^0 | \chi_j^c \rangle &= \delta_{ij} , & \langle \chi_i^0 | \chi_i^c \rangle &= 0 , \\ \langle \chi_i^c | \chi_j^c \rangle + \langle \chi_i^c | \chi_j^0 \rangle &= 0, & i, j &= 1, 2, \dots, N. \end{aligned} \quad \text{II.6}$$

The first condition is satisfied by using the Hartree-Fock orbitals for the unperturbed states. The second condition is satisfied automatically by angular symmetries since we are only considering dipole perturbations. The last condition was satisfied approximately for all positions of the perturbing charge by adjusting  $\lambda$  in the s $\rightarrow$ p and p $\rightarrow$ s equations. The remaining  $\lambda$  in the p $\rightarrow$ d equation was then adjusted such that the partial dipole polarizabilities [Eq. I.29], summed to the experimental value.

These conditions were observed to restrict the values of  $\lambda$  for each of the three transitions to a relatively unique triplet. Those chosen for this calculation are listed in Table VII. As may be observed from the values chosen, there is some arbitrariness in their choice. Although negative values would permit satisfying the conditions, they were not considered. Choosing two of the triplet values to be the same of course made satisfying the imposed conditions more difficult. The conditions also justified our approximating the exchange integral by  $A_s$ , as above, rather than the more complex combination  $(A_s - 3/2 A_s'')$  used for the electron scattering calculation in Part I. The perturbed orbitals, determined by using both forms for the approximation and satisfying the conditions discussed above with appropriate triplets, were then used to calculate a polarization potential given by Eq. I.32. The two potentials were found to be almost identical, hence the simpler approach was adopted.

We now conclude this discussion of the representation

of the initial and final states with a few comments regarding the bound valence and continuum states. Their determination reduces to a solution of an appropriate radial equation, which can be written as, using the notation defined in Eqs. I.31 through I.35,

$$(L+k^2)F_{kl}(R) = KF_{kl}(R) + \sum_m \int_0^{\infty} \tilde{u}_{m'l}(r') V_p(r') F_{kl}(r') dr' u_{ml}(R). \quad \text{II.7}$$

This equation serves to determine both the bound and continuum state reduced radial wave function. The continuum function,  $F_{kl} = u'_{kp}$ , is determined if  $k^2$  is taken as the kinetic energy of the scattered electron; or the bound state,  $F_{kl} = u'_{ns}$ , if  $k^2$  is taken as the binding energy. These are the perturbed functions, as is implied by the primes. The solution of the equation, with  $V_p = 0$ , are the unperturbed fixed-core Hartree-Fock (FCHF) functions and designated by the absence of the prime. The last term, which is summed over all occupied states, imposes the constraint that the continuum and bound state functions shall be orthogonal to the core states.

The calculated binding energies are tabulated and compared with experiment<sup>22</sup> in Table VIII. The non-coulomb phase shifts of the continuum wave functions are compared with those of others<sup>23,24,25</sup> in Table IX.

In the succeeding discussions, we refer to calculations using only FCHF wave functions and restricting the sum over  $p$  in Eq. II.2 to just the zero value, as the zeroth-order calculation. Matrix elements constructed with initial and final states of the form of Eq. II.2 are referred to as

first-order corrections, if the valence and continuum wave functions are taken as the solutions of Eq. II.7 with  $V_p = 0$ . The second-order corrections are those when the valence and continuum states are taken as the solutions of the full Eq. II.7.

### II-3. MATRIX ELEMENTS

In the dipole approximation, the valence electron ejected from the ground state of the sodium or potassium atom is in a p-wave state, and the expressions for the photoionization cross sections in the length and velocity forms are given by<sup>18</sup>

$$\sigma_L = 4/3 \pi \alpha a_0^2 (I + \epsilon) \sum_m |\vec{M}_{fi}^{(L)}|^2, \quad \text{II.8}$$

$$\sigma_V = 4/3 \pi \alpha a_0^2 (4/(I + \epsilon)) \sum_m |\vec{M}_{fi}^{(V)}|^2, \quad \text{II.9}$$

where  $I$  is the first ionization potential,  $\epsilon$  is the energy of the ejected electron,  $\alpha$  is the fine structure constant,

$$\vec{M}_{fi}^{(L,V)} = \int \Psi_f^* \sum_j \hat{O}_j^{(L,V)} \Psi_i d\tau, \quad \text{II.10}$$

and  $\hat{O}^L = \vec{r}$ ,  $\hat{O}^V = \vec{\nabla}$ . The summation is over final state orbital-projection quantum numbers.

The matrix elements are evaluated after inserting  $\phi_i = \phi_{ns}$  into Eq. II.2 for  $\Psi_i$ , and  $\phi_f = \phi_{kp}$  into Eq. II.2 for  $\Psi_f$ . The bound state function was normalized to one and the continuum to

$$\begin{aligned} \phi_{kp} &= r^{-1} u_k(r) Y_{1,m}(\vec{r}), \\ u_{kp}(r) &\xrightarrow{r \rightarrow \infty} k^{-1/2} \sin(kr - \pi/2 + \eta_1 + \sigma_1 + k^{-1} \ln 2kr) \end{aligned} \quad \text{II.11}$$

The constant  $4/3 \pi \alpha a_0^2 = 8.56 \times 10^{-19} \text{ cm}^2$  and the remaining quantities are taken in the system of atomic units  $\hbar = 1$ ,  $e^2 = 1/m = 2$ . The non-coulomb phase shift is  $\eta_1$ , and  $\sigma_1 = \arg \Gamma(2-i/k)$ , where  $\Gamma$  is the gamma function.

The matrix elements, keeping only terms linear in  $\chi'$ , are readily reduced and separable into components of different orders. The zeroth-order component of the matrix elements simplifies to

$$M^{(0)} = \langle \phi_{kp}^{\circ}(x) | \hat{\sigma}_x | \phi_{m0}^{\circ}(x) \rangle, \quad \text{II.12}$$

with all multiplicative overlaps equalling one.

The first-order component will have contributions from both the initial and final state corrections for each of the

three transitions.  $M^{(2)} = 2 \sum_m \langle \chi'_{n'p \rightarrow 0}(j; x) \phi_{kp}^{\circ}(x) | \hat{\sigma}_j | \chi_{n'p m}^{\circ}(j) \phi_{m0}^{\circ}(x) \rangle$

sition are

$$\begin{aligned} M^{(1)} = & 2 \langle \chi'_{n'0 \rightarrow p}(j; x) \phi_{kp}^{\circ}(x) | \hat{\sigma}_x | \chi_{n'p m}^{\circ}(x) \phi_{m0}^{\circ}(j) \rangle \\ & - \sum_m \langle \chi'_{n'p m \rightarrow 0}(j; x) \phi_{kp}^{\circ}(x) | \hat{\sigma}_x | \chi_{n'p m}^{\circ}(x) \phi_{m0}^{\circ}(j) \rangle \\ & - \langle \chi'_{n'0 \rightarrow p}(j; x) \phi_{kp}^{\circ}(x) | \hat{\sigma}_j | \chi_{n'p m \rightarrow 0}(j; x) \phi_{m0}^{\circ}(x) \rangle \\ & + 2 \sum_m \langle \chi_{n'p m}^{\circ}(j) \phi_{kp}^{\circ}(x) | \hat{\sigma}_j | \chi'_{n'p m \rightarrow 0}(j; x) \phi_{m0}^{\circ}(x) \rangle \\ & + 2 \langle \chi_{n'0}^{\circ}(j) \phi_{kp}^{\circ}(x) | \hat{\sigma}_j | \chi'_{n'0 \rightarrow p}(j; x) \phi_{m0}^{\circ}(x) \rangle \\ & - \langle \chi_{n'0}^{\circ}(j) \phi_{kp}^{\circ}(x) | \hat{\sigma}_j | \chi'_{n'0 \rightarrow p}(x; j) \phi_{m0}^{\circ}(j) \rangle \cdot \\ & - \langle \chi_{n'0}^{\circ}(j) \phi_{kp}^{\circ}(x) | \hat{\sigma}_j | \chi'_{n'0 \rightarrow p}(j; x) \phi_{m0}^{\circ}(j) \rangle \cdot \end{aligned} \quad \text{II.13}$$

The first pair of terms arise from the final state correction and the last pair from the initial state correction. The second of each pair is an exchange correction.

The similar set of terms for the p+s transition are

$$\begin{aligned} M^{(2)} = & 2 \sum_m \langle \chi'_{n'p \rightarrow 0}(j; x) \phi_{kp}^{\circ}(x) | \hat{\sigma}_j | \chi_{n'p m}^{\circ}(j) \phi_{m0}^{\circ}(x) \rangle \\ & - \sum_m \langle \chi'_{n'p m \rightarrow 0}(j; x) \phi_{kp}^{\circ}(x) | \hat{\sigma}_x | \chi_{n'p m}^{\circ}(x) \phi_{m0}^{\circ}(j) \rangle \\ & + 2 \sum_m \langle \chi_{n'p m}^{\circ}(j) \phi_{kp}^{\circ}(x) | \hat{\sigma}_j | \chi'_{n'p m \rightarrow 0}(j; x) \phi_{m0}^{\circ}(x) \rangle \end{aligned}$$

$$-\sum_m \langle \chi_{n',p,m}^o(j) \phi_{kp}^o(x) | \hat{\mathcal{O}}_x | \chi_{n',p,m \rightarrow d}^o(x;j) \phi_{n'o}^o(x) \rangle. \quad \text{II.14}$$

The first two terms are due to the final state correction and the last two from the initial state correction.

The contributions arising from the  $p \rightarrow d$  transition are

$$\begin{aligned} M^{(3)} = & 2 \sum_m \langle \chi_{n',p,m \rightarrow d}^o(j;x) \phi_{kp}^o(x) | \hat{\mathcal{O}}_j | \chi_{n',p,m}^o(j) \phi_{n'o}^o(x) \rangle \\ & + 2 \sum_m \langle \chi_{n',p,m}^o(j) \phi_{kp}^o(x) | \hat{\mathcal{O}}_j | \chi_{n',p,m \rightarrow d}^o(j;x) \phi_{n'o}^o(x) \rangle \\ & - \sum_m \langle \chi_{n',p,m}^o(j) \phi_{kp}^o(x) | \hat{\mathcal{O}}_x | \chi_{n',p,m \rightarrow d}^o(x;j) \phi_{n'o}^o(j) \rangle. \end{aligned} \quad \text{II.15}$$

There is no exchange term in the final state correction. The last two are again the terms due to the initial state correction.

The evaluation of the matrix elements is simplified by the vanishing of both the x and y-components of the vector operator. A further simplification arises in evaluating the z-component. The dependence on m of the three possible final states is associated with the angular coordinates; and their evaluation yields identical multiplicative factors for the radial integrals,<sup>26</sup> which have to be evaluated numerically. The summation over the final states thus contributes a factor of three to the multiplicative constant. Finally, the  $p \rightarrow d$  initial state exchange term vanishes on angular integration. Below, W and u will represent respectively the reduced radial functions for the perturbed orbital and unperturbed functions. The sum of the z-components of the matrix elements becomes



$$(M_{fi})_2 = \int (\bar{\mathcal{O}}_0^+ \psi_{m_0}(1)) \psi_{kp}(1) d\lambda_1 \quad \text{II.16 A}$$

$$+ \frac{2}{3} \iint W_{m_0 \rightarrow p}^{(1;2)} (\bar{\mathcal{O}}_1^+ (1) \psi_{m_0}(1)) d\lambda_1 \psi_{m_0}(2) \psi_{kp}(2) d\lambda_2 \quad \text{II.16 B}$$

$$- \frac{1}{3} \iint W_{m_0 \rightarrow p}^{(2;1)} \psi_{m_0}(1) (\bar{\mathcal{O}}_1^+ (1) \psi_{m_0}(1)) d\lambda_1 \psi_{kp}(2) d\lambda_2 \quad \text{II.16 C}$$

$$+ \frac{2}{3} \iint W_{m_0 \rightarrow p}^{(1;2)} (\bar{\mathcal{O}}_0^+ (1) \psi_{m_0}(1)) d\lambda_1 \psi_{m_0}(2) \psi_{kp}(2) d\lambda_2 \quad \text{II.16 D}$$

$$- \frac{1}{3} \iint W_{m_0 \rightarrow p}^{(2;1)} \psi_{m_0}(1) \psi_{m_0}(1) (\bar{\mathcal{O}}_0^+ (2) \psi_{kp}(2)) d\lambda_2 \quad \text{II.16 E}$$

$$- \frac{4}{3} \iint W_{m_0 \rightarrow p}^{(1;2)} (\bar{\mathcal{O}}_2^+ (1) \psi_{m_0}(1)) d\lambda_1 \psi_{m_0}(2) \psi_{kp}(2) d\lambda_2 \quad \text{II.16 F}$$

$$+ \frac{2}{3} \iint W_{m_0 \rightarrow p}^{(1;2)} (\bar{\mathcal{O}}_0^+ (1) \psi_{m_0}(1)) d\lambda_1 \psi_{m_0}(2) \psi_{kp}(2) d\lambda_2 \quad \text{II.16 G}$$

$$- \frac{1}{3} \iint W_{m_0 \rightarrow p}^{(1;2)} (\bar{\mathcal{O}}_0 (1) \psi_{m_0}(1)) d\lambda_1 \psi_{m_0}(2) \psi_{kp}(2) d\lambda_2 \quad \text{II.16 H}$$

$$+ \frac{2}{3} \iint W_{m_0 \rightarrow p}^{(1;2)} (\bar{\mathcal{O}}_1^- (1) \psi_{m_0}(1)) d\lambda_1 \psi_{m_0}(2) \psi_{kp}(2) d\lambda_2 \quad \text{II.16 I}$$

$$- \frac{1}{3} \iint W_{m_0 \rightarrow p}^{(1;2)} \psi_{m_0}(1) d\lambda_1 (\bar{\mathcal{O}}_1^- (2) \psi_{m_0}(2)) \psi_{kp}(2) d\lambda_2 \quad \text{II.16 J}$$

$$+ \frac{4}{3} \iint W_{m_0 \rightarrow p}^{(1;2)} (\bar{\mathcal{O}}_1^+ (1) \psi_{m_0}(1)) d\lambda_1 \psi_{m_0}(2) \psi_{kp}(2) d\lambda_2 \quad \text{II.16 K}$$

The operators in the integrals will be dependent on whether the dipole-length or dipole-velocity approximation is being considered. Their form is determined by the notation

$$\begin{aligned} \text{length: } \bar{\mathcal{O}}_l^{\pm} &= \bar{\mathcal{O}}_l^{\pm} = r, \\ \bar{\mathcal{O}}_l^{\pm} &= \frac{d}{dx} \mp \frac{\{l^{\pm+1}\}}{r} \\ \text{velocity: } \bar{\mathcal{O}}_l^{\pm} &= -\frac{d}{dx} \mp \frac{\{l^{\pm+1}\}}{r}. \end{aligned} \quad \text{II.17}$$

The choice of  $l$  or  $l+1$  is associated respectively with the upper + or lower - sign.

One last consideration is the second-order corrections. These are obtained from the zeroth-order integrals by replacement of the unperturbed reduced radial functions for the valence and continuum states by the corresponding perturbed functions. The subscripts on the reduced radial function representing the perturbed orbital indicates the transition being considered. The five integrals after the first correspond to the final state correction and the last five to the initial state correction.

## II-4. RESULTS

The contributions from the integrals are combined and listed in Table X for sodium and Table XI for potassium. The columns labeled L or V respectively signify that their values were obtained by using the length or velocity operators in the integrals. When the velocity operator is used some of the integrals will cancel; for example, the sum of the integrals II.16 B, C, G and H give the values listed in  $L1_{s \rightarrow p}$ , but only the integrals II.16 C and H will sum to the values listed in  $V1_{s \rightarrow p}$ . Similarly the sum of the integrals II.16 D, E, I and J appears in the column  $L1_{p \rightarrow s}$ , while just the integrals II.16 E and J sum to the value in column  $V1_{p \rightarrow s}$ . The values in columns L0 and V0 are those of the integral II.16 A and those in  $L1_{p \rightarrow d}$  are the sum of the integrals II.16 F and K.

The second-order corrections listed in columns L2 and V2 are obtained by taking the difference between

$$\int (\bar{\phi}_0^+ u'_{n0}(\gamma)) u'_{kp}(\gamma) d\gamma, \quad \text{II.18 A}$$

and

$$\int (\bar{\phi}_0^+ u_{n0}(\gamma)) u_{kp}(\gamma) d\gamma. \quad \text{II.18 B}$$

The most prominent aspect of the values of the first-order correction is that they exceed those of the zeroth-order near threshold. The first-order contributions from the  $L1_{s \rightarrow p}$  compensate those of the  $L1_{p \rightarrow s}$  as is expected, but the large  $L1_{p \rightarrow d}$  values remain to overwhelm the zeroth-order values. There is no  $p \rightarrow d$  contribution in the velocity case, and the cancellation between the  $s \rightarrow p$  and  $p \rightarrow s$  is less satis-

factory.

The plot of the photoionization cross section of zero-order and first-order are given in Fig. 3 for sodium and Fig. 4 for potassium. The agreement between the zero-order length and velocity curves are good except for the relative displacement of their minima. The disruptive effect of the first-order correction destroys the approximate agreement of the length and velocity curves that existed in zero-order.

The dipole-length and dipole-velocity curves for the total photoionization cross section correct to second order are shown in Fig. 5 for sodium and Fig. 6 for potassium. In these figures are included for comparison the experimental points of Hudson and Carter<sup>26</sup> and the recent calculations of Weisheit.<sup>27</sup> Also shown in Figures 5 and 6 are the adiabatic-exchange-dipole (AED) approximation results given by Eq. II.18 A. The AED results for sodium are in agreement with those of Boyd<sup>28</sup> who used the AED approach for her analysis. Only a slight improvement in the agreement of the length and velocity curves is seen for the potassium AED results. The vertical bars represent the deviations between the length and velocity calculations.

The good agreement of the AED results for sodium but not for potassium was considered to be due to the failure to satisfy the orthogonality condition to as high a degree as was done for sodium. An additional calculation for potassium was performed and the orthogonality condition was best satisfied by choosing the same value (0.444139) in both the  $s \rightarrow p$  and  $p \rightarrow s$

equations. However, in order to satisfy the experimental value of the dipole polarizability, the  $\lambda$  value for the  $p \rightarrow d$  transition had to be negative (-0.68600). This yielded a total polarizability of  $5.470 \text{ a}_0^3$ . This triplet of values gave a better binding energy for the  $4s$  state (-0.32227); and the non-coulomb phase shifts were: 2.285, 2.221, 2.199, 2.148 respectively for the  $k$  values 0.000, 0.300, 0.350, 0.450.

The negative value presents an interpretive difficulty. More drastic, however, was the effect on the photoionization cross section. Both the length and velocity curves showed minima, relatively displaced; but their values over the entire energy range considered were depressed below  $0.67 \times 10^{-20} \text{ cm}^2$ .

## II-5. CONCLUSIONS

In their analysis of the lithium atom, Matese and LaBahn<sup>1</sup> were successful in calculating photoionization cross sections to different orders, up to the second. Using the polarized orbital method they were able to improve on their initial and final state representation and obtained better agreement between the dipole-length and dipole-velocity curves and also with experiment.

The application of their analysis here to sodium and potassium failed because of the large value of the first-order corrections. The first-order correction is on the order of and larger than the zero-order value whereas for lithium it was lower by an order of magnitude. The non-cancellation of the  $p \rightarrow d$  first-order contribution may indicate that this method is applicable only to atomic systems containing s-type electrons.

There was no attempt made to fit the experimental curve by varying the adjustable parameter. This would be contrary to the nature of the procedure, i.e., to predict the shape of the curve. Weisheit using a different approach was able to reproduce a portion of the photoionization curve with an effective dipole operator containing a cut-off parameter, provided he had knowledge of the location of the minimum or the value at threshold.

The fortuitous agreement of the AED curves, with those of Weisheit does not justify the conclusion that the final and initial states are correctly represented in the AED

approximation.

Sufficient agreement of specific results of this calculation with those of others confirms our faith in the absence of any significant errors in the computer programs. With the failure of the cross sections to behave in the same manner as illustrated by lithium, we have to conclude that the procedure cannot be relied upon to predict the interaction of complex atoms with radiation.

TABLE VII: Contributions to the dipole polarizability (in  $a_0^3$ )  
associated with the adjustable parameters

	Sodium		Potassium	
	$\lambda$	$\alpha$	$\lambda$	$\alpha$
ns $\rightarrow$ p	0.53070	0.8894	0.78036	7.4887
np $\rightarrow$ s	0.25094	-0.7704	0.10477	-8.5280
np $\rightarrow$ d	0.20000	0.8592	0.10477	6.5110
Total		0.9782		5.4717
Experimental <sup>a</sup>		0.978		5.47

<sup>a</sup> Öpik (Ref. 30)



TABLE VIII: Calculated valence-electron binding energies  
and experimental ionization energy (I)

Approximation	Sodium	Potassium
Neutral atom <sup>a</sup>	-0.36422	-0.29484
FCHF	-0.36363	-0.29382
AED	-0.38196	-0.33281
Experimental (I) <sup>b</sup>	0.37773	0.31904

<sup>a</sup> Clementi (Ref. 10)

<sup>b</sup> Ham (Ref. 22)

TABLE IX: Non-coulomb p-wave phase shifts (in rad.)

Element	k	k <sup>2</sup>	Present	Pseudopotential	Quantum Defect
Na	0.000	0.00	2.728	2.684 <sup>a</sup>	2.687 <sup>b</sup>
	0.300	0.09	2.698		
	0.316	0.10		2.650	2.656
	0.350	0.12	2.688		
	0.450	0.20	2.663	2.618	2.632
K	0.000	0.00	2.362	2.235	2.234 <sup>c</sup>
	0.300	0.09	2.298		
	0.316	0.10		2.164	2.152
	0.350	0.12	2.277		
	0.450	0.20	2.227	2.100	2.070

<sup>a</sup> Smith and LaBahn (Ref. 23)

<sup>b</sup> Seaton (Ref. 24)

<sup>c</sup> Burgess and Seaton (Ref. 25)

TABLE X: Sodium zeroth-order matrix elements and corrections of first- and second-order in the length (L) and velocity (V) forms for the transitions  $s \rightarrow p$ ,  $p \rightarrow s$ , and  $p \rightarrow d$

k	L0	L1 <sub>s→p</sub>	L1 <sub>p→s</sub>	L1 <sub>p→d</sub>	L2	V0	V1 <sub>s→p</sub>	V1 <sub>p→s</sub>	V2
0.00	-0.549	0.177	-0.187	0.150	-0.014	0.087	0.010	-0.002	0.017
0.01	-0.450	0.175	-0.186	0.148	-0.017	0.071	0.010	-0.002	0.017
0.02	-0.214	0.171	-0.182	0.144	-0.022	0.030	0.010	-0.002	0.016
0.03	0.042	0.164	-0.176	0.137	-0.021	-0.022	0.010	-0.002	0.014
0.04	0.232	0.156	-0.169	0.129	-0.013	-0.073	0.011	-0.002	0.011
0.05	0.337	0.148	-0.162	0.120	-0.002	-0.115	0.010	-0.003	0.008
0.06	0.373	0.138	-0.153	0.111	0.008	-0.147	0.010	-0.003	0.004
0.07	0.367	0.129	-0.145	0.102	0.015	-0.168	0.010	-0.004	0.000
0.08	0.340	0.120	-0.137	0.093	0.020	-0.181	0.010	-0.004	-0.003
0.09	0.304	0.112	-0.129	0.085	0.022	-0.188	0.010	-0.005	-0.006

TABLE XI: Potassium zeroth-order matrix elements and corrections of first- and second-order in the length (L) and velocity (V) forms for the transition  $s \rightarrow p$ ,  $p \rightarrow s$ , and  $p \rightarrow d$

k	L0	$L1_{s \rightarrow p}$	$L1_{p \rightarrow s}$	$L1_{p \rightarrow d}$	L2	V0	$V1_{s \rightarrow p}$	$V1_{p \rightarrow s}$	V2
0.00	-0.430	0.938	-1.106	0.723	-0.063	0.031	0.049	-0.011	0.061
0.01	-0.324	0.927	-1.093	0.713	-0.068	0.017	0.049	-0.011	0.060
0.02	-0.084	0.895	-1.058	0.686	-0.071	-0.018	0.049	-0.011	0.057
0.03	0.145	0.849	-1.004	0.645	-0.054	-0.059	0.049	-0.011	0.051
0.04	0.286	0.795	-0.941	0.596	-0.022	-0.095	0.048	-0.012	0.042
0.05	0.339	0.738	-0.875	0.545	0.013	-0.122	0.048	-0.013	0.032
0.06	0.336	0.681	-0.808	0.494	0.040	-0.138	0.048	-0.014	0.021
0.07	0.307	0.626	-0.743	0.446	0.057	-0.147	0.047	-0.015	0.012
0.08	0.270	0.574	-0.683	0.401	0.065	-0.150	0.046	-0.016	0.004
0.09	0.233	0.526	-0.626	0.359	0.068	-0.151	0.044	-0.018	-0.004

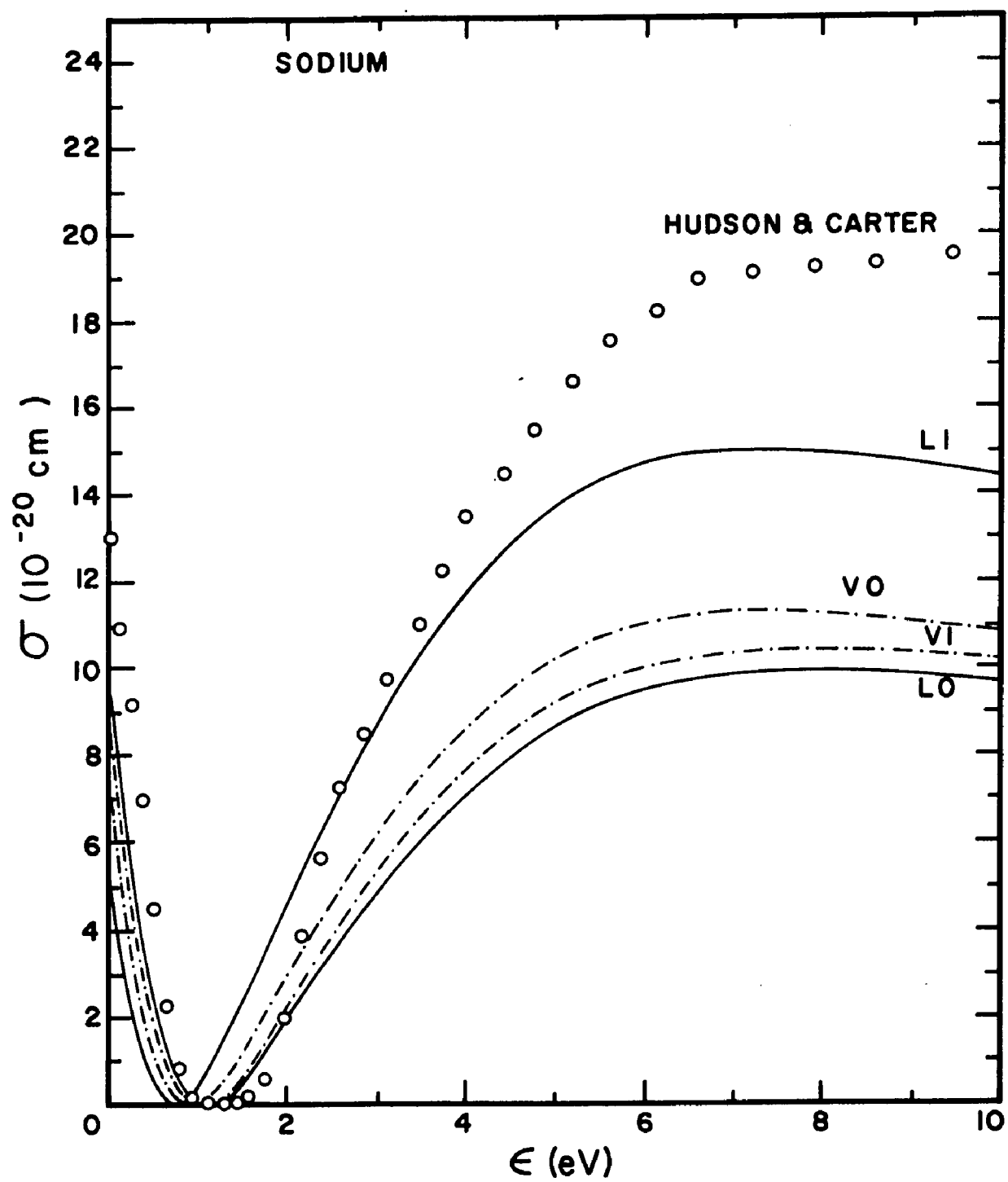
## FIGURE CAPTIONS

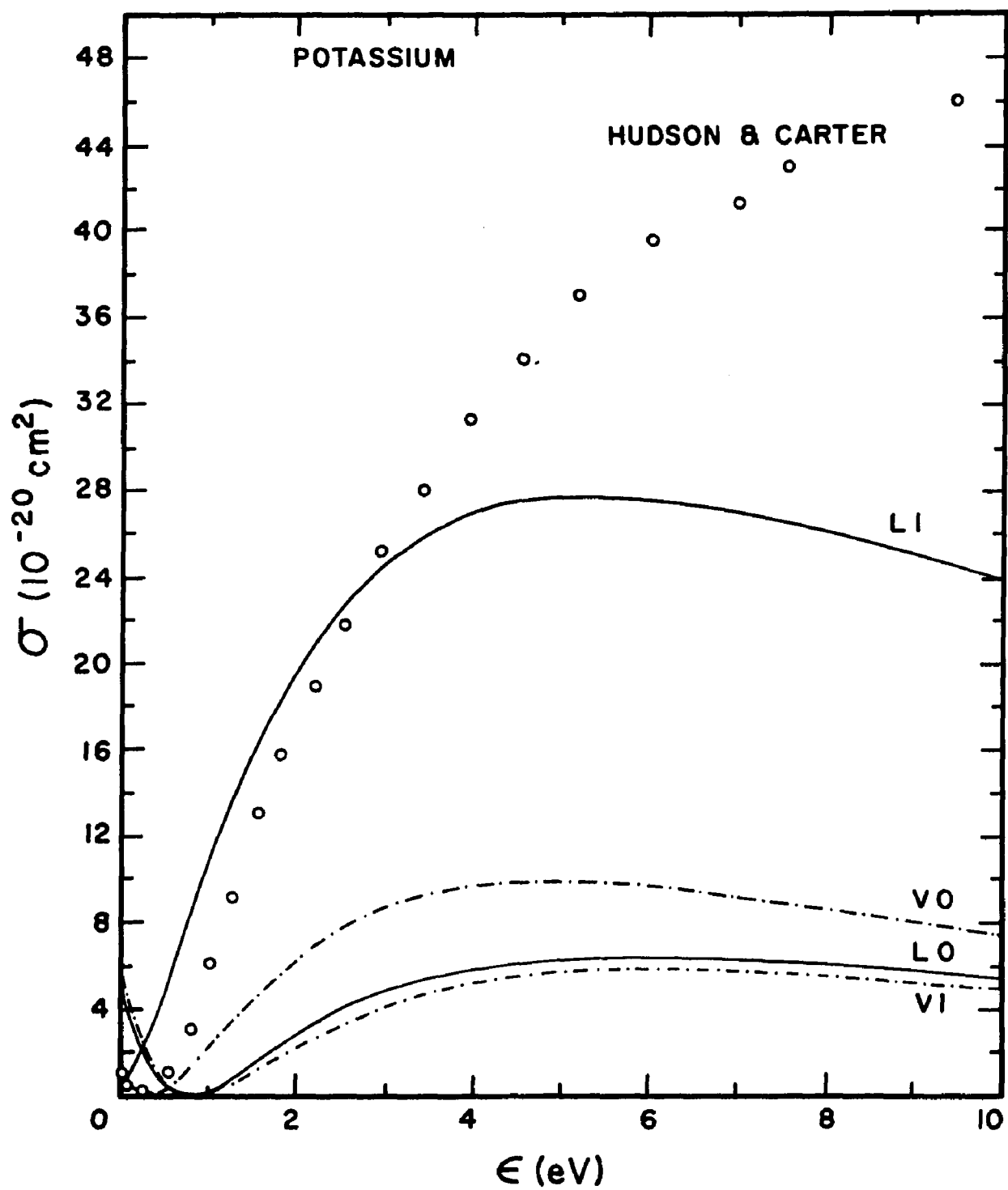
Figure 3: Photoionization cross sections for sodium. L0 and V0 are Hartree-Fock calculations in the length and velocity forms, respectively. L1 and V1 included first-order corrections as explained in the text.

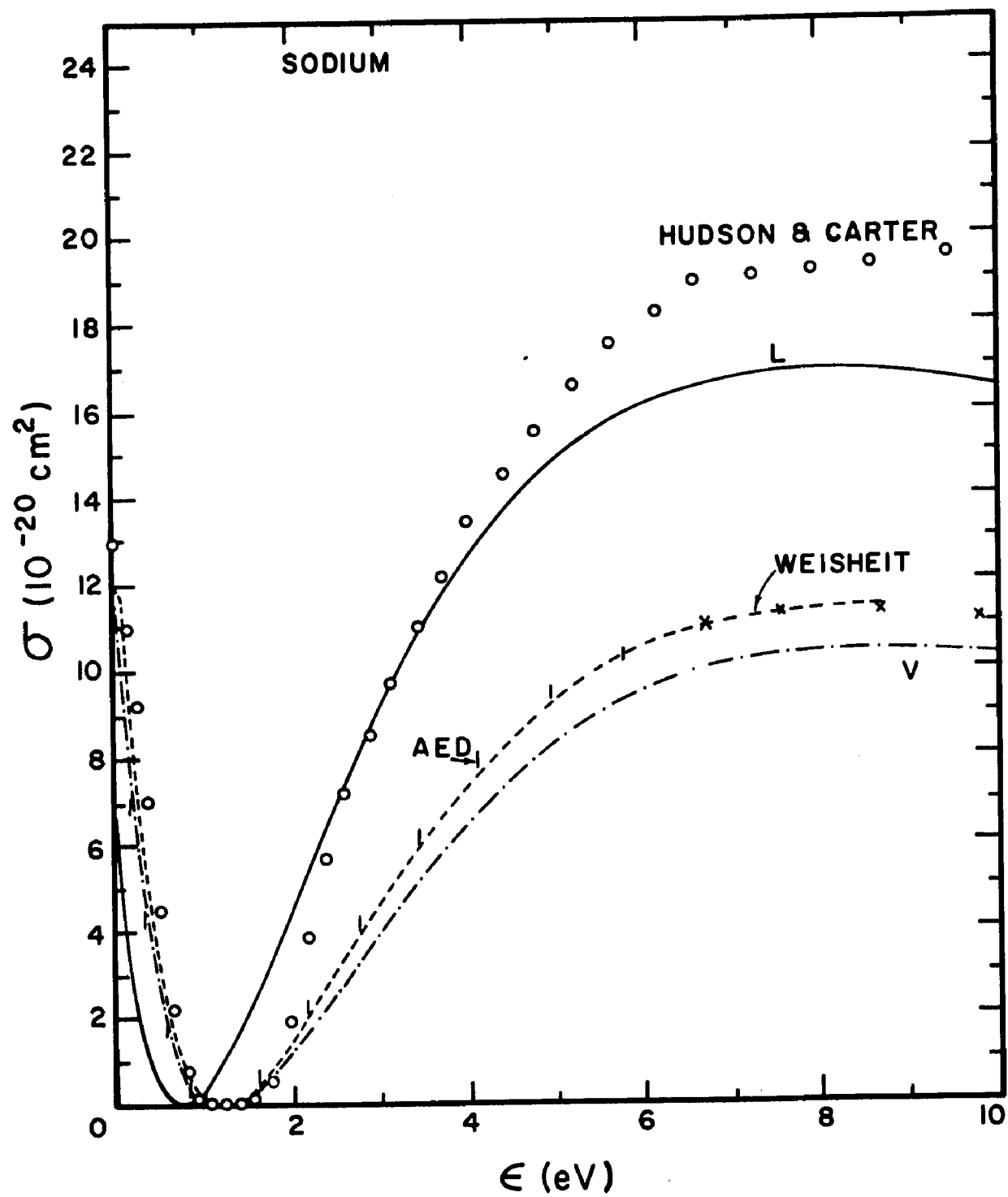
Figure 4: Photoionization cross sections for potassium. L0 and V0 are Hartree-Fock calculations in the length and velocity forms, respectively, L1 and V1 included first-order corrections as explained in the text.

Figure 5: Photoionization cross sections for sodium. L and V indicate respectively the final length and velocity calculations of this work. The circles are the experimental data (Ref. 27) and dashed curve are recent calculations by Weisheit (Ref. 28).

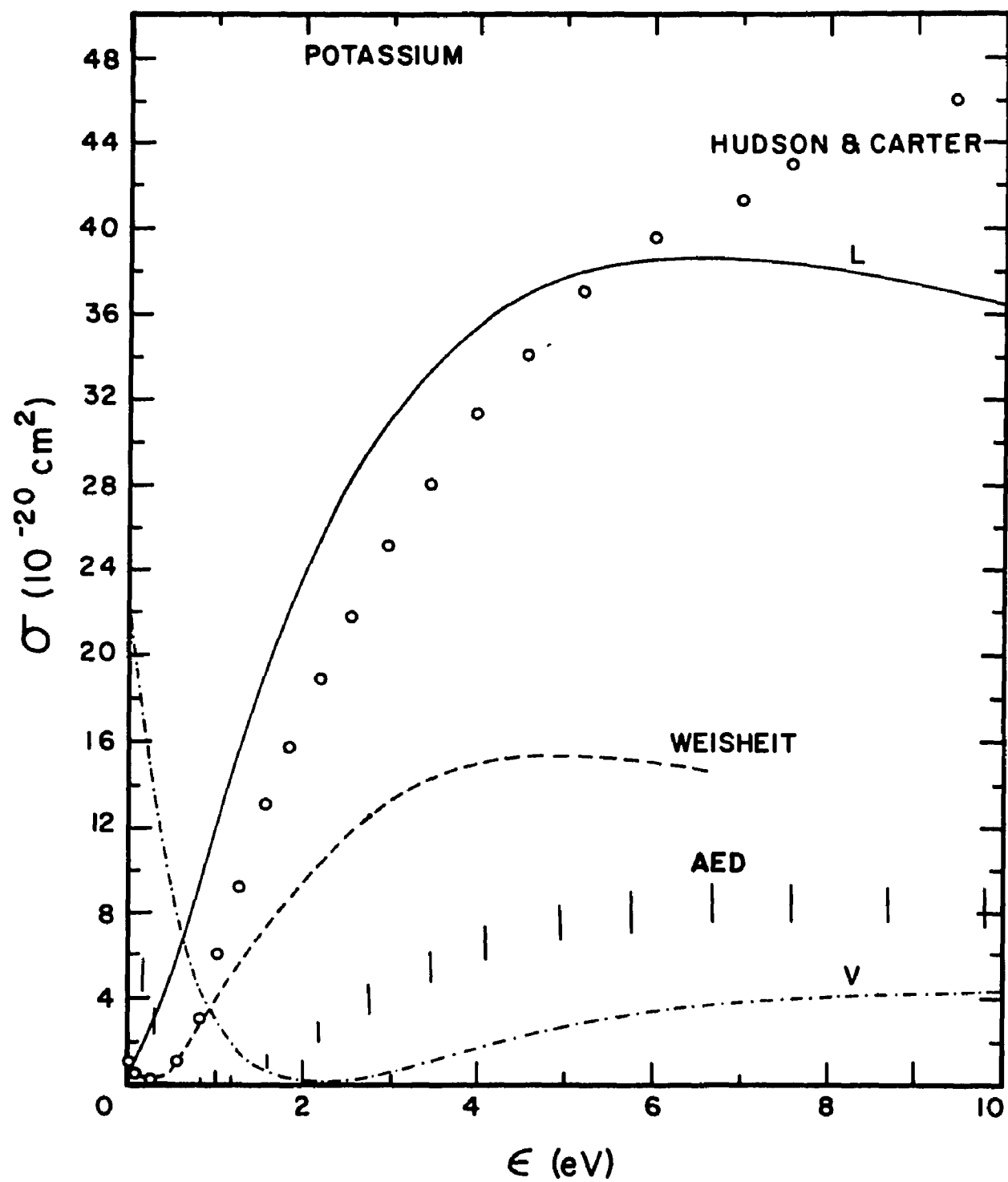
Figure 6: Photoionization cross sections for potassium. L and V indicate respectively the final length and velocity calculations of this work. The circles are the experimental data (Ref. 27) and dashed curve are recent calculations by Weisheit (Ref. 28).











## REFERENCES

1. J. J. Matese and R. W. LaBahn, Phys. Rev. 188, 17 (1969).
2. R. W. LaBahn and J. Callaway, Phys. Rev. 135, A1539 (1964).
3. R. W. LaBahn and J. Callaway, Phys. Rev. 147, 28 (1966).
4. A. Temkin. Phys. Rev. 107, 1004 (1957).
5. D. G. Thompson, Proc. Roy. Soc. A, 294, 160 (1966).
6. The notation used in this section is that of Langhoff, Karplus, and Hurst<sup>7</sup> with minor modifications. One modification corresponds to the use of the set of atomic units where  $\hbar=1$ , and  $e^2=1/m=2$  (energies in rydbergs).
7. Langhoff, Karplus, and Hurst, J. Chem. Phys. 44, 505 (1966).
8. A. Dalgarno, Advan. Phys. 11, 281 (1962).
9. R. M. Sternheimer, Phys. Rev. 96, 951 (1954).
10. E. Clementi, IBM Journal 9, 2 (1965).
11. J. C. Slater. "Quantum Theory of Atomic Structure", (McGraw-Hill, New York, 1960), Vol. II, p. 14.
12. A. Burgess, Proc. Phys. Soc. 81, 442 (1962).
13. S. Kaneko, J. Phys. Soc. Japan 14, 1600 (1959).
14. R. E. Montgomery and R. W. LaBahn, Can. J. Phys. 48, 1287 (1970).
15. W. Kohn and L. J. Sham, Phys. Rev. 140, A1133 (1965).
16. A. Salop and H. H. Nakano, Phys. Rev. A2, 127 (1970).
17. D. E. Golden and H. W. Bandel, Phys. Rev. 149, 58 (1966).
18. H. A. Bethe and E. F. Salpeter, "Quantum Mechanics of One- and Two-Electron Atoms" (Academic Press Inc., New

York, 1957) pgs. 248 and 295.

19. S. Chandrasekhar, *Astrophys. J.* 102, 223 (1945).
20. E. S. Chang and M. R. C. McDowell, *Phys. Rev.* 176, 126 (1968).
21. L. C. Allen, *Phys. Rev.* 118, 167 (1960).
22. F. S. Ham, "Solid State Physics". edited by F. Seitz and D. Turnbull (Academic Press, New York, 1955), Vol. 1, p. 127.
23. R. L. Smith and R. W. LaBahn, *Phys. Rev.* A2, 2317 (1970).
24. M. J. Seaton, *Proc. Phys. Soc. (London)* A70, 620 (1957).
25. A. Burgess and M. J. Seaton, *Mon. Not. Roy. Astr. Soc.* 120, 121 (1960).
26. M. Mizushima, "Quantum Mechanics of Atomic Spectra and Atomic Structure" (W. A. Benjamin, New York, 1970) p.119.
27. R. D. Hudson and V. L. Carter, *J. Opt. Soc. Amer.* 57, 651 and 1471 (1967).
28. J. C. Weisheit, *Phys. Rev.* A5, 1621 (1972).
29. A. H. Boyd, *Planet Space Sci.* 12, 729 (1964).
30. U. Opik, *Proc. Phys. Soc. (London)* 92, 566 (1967).

## VITA

Edward Andrew Garbaty, son of Anthony and Nellie Garbaty was born in Jersey City, New Jersey on November 30, 1930. He graduated from North Arlington High School in New Jersey in 1948. He studied physics at the Newark Colleges of Rutgers University, and received an A. B. degree in 1953. He then served two years with the U. S. Army Signal Corp. After Service he entered the Graduate School of Iowa State University and in 1959 received a M. S. degree in physics. In succession he held posts as instructor for two years at Loras College, Dubuque, Iowa; a year appointment at TriState College, Angola, Indiana; and after four years held the rank of associate professor at the State University of New York at Geneseo. Before taking the position at Geneseo, he married Caroline Becker of Dayton, Ohio; who while at Geneseo gave birth to a daughter, a son, and twin daughters. He brought them to Baton Rouge in the Fall of 1966, to earn a Ph. D. degree at Louisiana State University. He left LSU in August, 1971 without the degree to take a position at Saint John's University, Collegeville, Minnesota. Caroline did not leave empty-handed, with two sons born to her while in Baton Rouge. Currently Edward A. Garbaty is a candidate for the degree of Doctor of Philosophy in the Department of Physics and Astronomy at the 1972 Fall Commencement.